ACS Medicinal Chemistry Letters

Letter

Discovery of Substituted 1H-Pyrazolo[3,4-b]pyridine Derivatives as Potent and Selective FGFR Kinase Inhibitors

Bin Zhao, Yixuan Li, Pan Xu, Yang Dai, Cheng Luo, Yiming Sun, Jing Ai, Mei-Yu Geng, and Wenhu Duan

ACS Med. Chem. Lett., **Just Accepted Manuscript** • DOI: 10.1021/acsmedchemlett.6b00066 • Publication Date (Web): 20 Apr 2016

ACS Publications

ACS Medicinal Chemistry Letters is published by the American Chemical Society. 1155 Sixteenth Street N.W., Washington, DC 20036

Discovery of Substituted 1*H*-Pyrazolo[3,4-*b*]pyridine Derivatives as Potent and Selective FGFR Kinase Inhibitors

Bin Zhao[†,∥], Yixuan Li[‡,∥], Pan Xu[§], Yang Dai[‡], Cheng Luo[§], Yiming Sun[‡], Jing Ai*[,‡], Meiyu Geng*[,‡], Wenhu Duan*[,†]

[†]Department of Medicinal Chemistry, [‡]Division of Antitumor Pharmacology, and [§]Drug Discovery and Design Center, State Key Laboratory of Drug Research, Shanghai Institute of Materia Medica, Chinese Academy of Sciences, 555 Zu Chong Zhi Road, Shanghai 201203, China

KEYWORDS: cancer, FGFR, inhibitor, pyrazolo[3,4-b]pyridine

ABSTRACT: Fibroblast growth factor receptors (FGFRs) are important targets for cancer therapy. Herein, we describe the design, synthesis, and biological evaluation of a novel series of 1*H*-pyrazolo[3,4-*b*]pyridine derivatives as potent and selective FGFR kinase inhibitors. On the basis of its excellent *in vitro* potency and favorable pharmacokinetic properties, compound **7n** was selected for *in vivo* evaluation and showed significant antitumor activity in a FGFR1-driven H1581 xenograft model. These results indicated that **7n** would be a promising candidate for further drug development.

Fibroblast growth factors (FGFs) and their receptors regulate a wide range of biological functions, including embryogenesis, tissue repair, wound healing, and angiogenesis.[1-3] The fibroblast growth factor receptor (FGFR) family comprises four highly conserved transmembrane tyrosine kinase receptors (FGFR1–4), which are differentially activated by binding to a subset of 18 FGF ligands.[3-4] Upon FGF binding, FGFR undergoes dimerization and auto phosphorylation, resulting in activation of downstream signaling pathways, such as the MAPK and PLCγ pathways.[4-5] These FGFR cascades play crucial roles in key cell behaviors, such as proliferation, survival, differentiation, and migration, which makes FGFR signaling susceptible to subversion by cancer cells.[6] Dysregulation of FGFR signaling has been documented in clinical samples of bladder, lung, breast cancers, etc,[7] and aberrant FGFR activation is closely correlated with metastatic progression and poor prognosis.[8-9] Knockdown studies and pharmaceutical inhibition of FGFRs in preclinical models have further demonstrated that FGFRs are attractive targets for cancer therapy.[4,7,10]

In recent years, many small molecules have been in clinical development, such as nintedanib, dovitinib, and cediranib, which are reported to target FGFR.[11] However, because of the high degree of homology of FGFRs with VEGFRs, most of these compounds have multitarget specificity, which leads to undesired side effects in their anticancer therapies.[12-13] Thus, discovery of highly selective FGFR inhibitors is an unmet medical need. Currently, several selective FGFR inhibitors have progressed robustly into clinical trials, such as NVP-BGJ398,[14] AZD4547,[15] and CH5183284[16] (Figure 1).

PD173074 (Figure 1), the first reported selective FGFR inhibitor, inhibits FGFR1 with an IC_{50} value of 21.5 nM at the molecular level, while inhibiting PDGFR, c-Src and EGFR, as well as several serine/threonine kinases with 1000-fold or

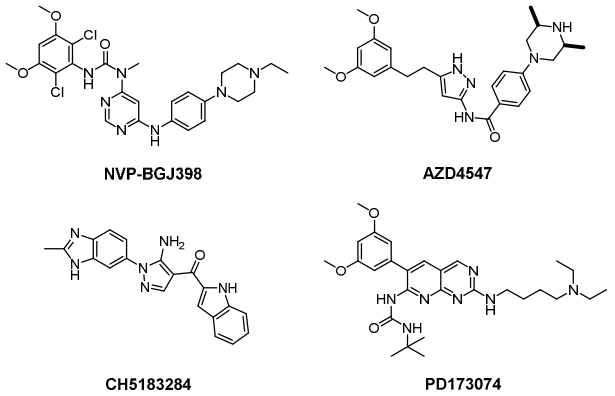

Figure 1. Structures of selective FGFR inhibitors.

greater IC_{50} values.[17] Nevertheless, PD173074 exhibits submicromolar inhibitory activity at the cellular level against VEGFR2 (IC_{50} = 100–200 nM).[17] The crystal structure of PD173074 in complex with the FGFR1 kinase domain elucidates that its high affinity and selectivity for FGFR1 stem from the presence of 3,5-dimethoxy phenyl ring that adopts an almost perpendicular orientation to the plane of the pyrido[2,3-*d*]pyrimidine rings and fills optimally a complementary hydrophobic pocket.[17] Guagnano *et al.* took advantage of this finding and then developed a selective FGFR inhibitor, NVP-

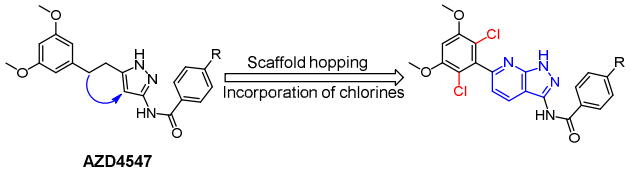

Figure 2. Design of novel FGFR inhibitors.

Scheme 1. Synthesis of Compounds 4a–k and 5[a]

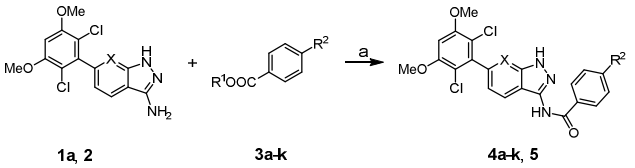

[a]Reagents and conditions: (a) $AlMe_3$, toluene, rt to 60 °C, 4%–28%.

Scheme 2. Synthesis of Compounds 7a–o, 9, 10, and 11a–c[a]

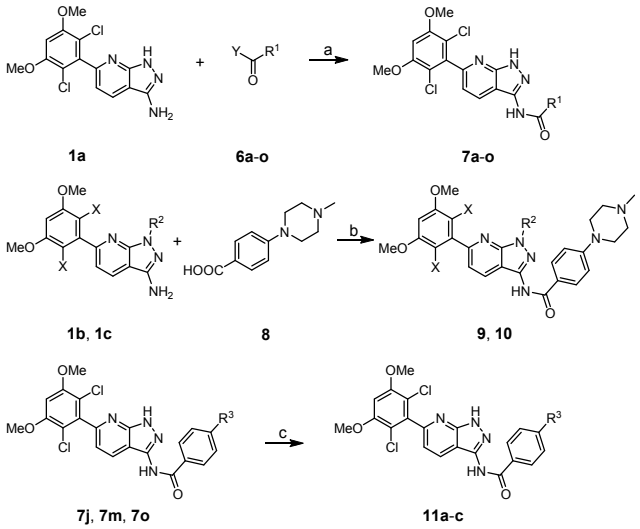

[a]Reagents and conditions: (a) for **7i** and **7k**, DIPEA, THF, 0 °C to rt, 38%–41%; for **7a**–**h**, **7j**, and **7l**–**o**, (i) oxalyl chloride, DMF, CH_2Cl_2, 0 °C to rt; (ii) DIPEA, THF, 0 °C to rt, 18%–60%; (b) (i) oxalyl chloride, DMF, CH_2Cl_2, 0 °C to rt; (ii) DIPEA, THF, 0 °C to rt, 59%–69%; (c) for **11a** and **11b**, CF_3COOH, CH_2Cl_2, rt, 83%–89%; for **11c**, TBAF, THF, 0 °C to rt, 56%.

BGJ398. NVP-BGJ398, currently in phase II clinical trials, inhibits FGFR1–4 (IC_{50} = 0.9, 1.4, 1.0, and 60 nM, respectively) with low nanomolar potency at the molecular level and has a minimum of 200-fold selectivity for FGFR1 over all other kinases evaluated (VEGFR2, IC_{50} = 180 nM).[14] The cocrystal structure of NVP-BGJ398 with FGFR1 elucidates that its higher potency and selectivity compared to PD173074 result from incorporation of chlorines at the 2- and 6-positions of the phenyl ring. The two chlorine atoms of NVP-BGJ398 enforce the plane of the phenyl ring adopting an almost perpendicular orientation to the plane of the pseudobicyclic system consisting of an *N*-pyrimidin-4-yl moiety; this conformation is closer to the kinase bound conformation; therefore, incorporation of chlorines decreases the deconjugation energy required to achieve the optimal binding conformation and thus enhances the potency of this scaffold.[14] Besides, the two chlorine atoms have favorable contacts with the gate keeper Val561 and Ala640 in FGFR1, respectively, while the Ala640 residue is replaced by a cysteine residue in VEGFR2.[14] The increased steric hindrance of cysteine compared to alanine might be the determinant of selectivity of the compound against VEGFR2.[14] AZD4547, an investigational drug in phase II clinical trials, has excellent *in vivo* efficacy and favorable pharmacokinetic properties. AZD4547 inhibits FGFR1–4 (IC_{50} = 0.2, 2.5, 1.8, and 165 nM, respectively) with low nanomolar potency at the molecular level, while inhibiting VEGFR2 with an IC_{50} value of 24 nM.[15] Based on these findings, we wished to explore new scaffolds based on the structure of AZD4547, which had higher potency and higher selectivity for FGFR over VEGFR2 than AZD4547. By utilizing the scaffold hopping strategy and incorporation of chlorines at the 2- and 6-positions of the phenyl ring, we designed novel 1*H*-pyrazolo[3,4-*b*]pyridine scaffold derivatives (Figure 2), which demonstrated excellent *in vitro* and *in vivo* antitumor activities and high selectivity for FGFR over VEGFR2. Herein, we report the synthesis and biological evaluation of these compounds.

As outlined in Schemes 1 and 2 (see Supporting Information Schemes S4 and S5 for details), two synthetic routes were employed for preparation of target compounds. Scheme 1 illustrates the synthesis of compounds **4a**–**k** and **5**, which were obtained by condensation of the appropriate amines (**1a** and **2**) and various substituted benzoic acid esters (**3a**–**k**) in the presence of trimethylaluminium at 60 °C. However, the yields of compounds **4a**–**k** and **5** synthesized via this route were unsatisfactory (4%–28%). Therefore, an alternative procedure was used to prepare **7a**–**o**, **9**, and **10** (Scheme 2). Various acyl chlorides, prepared from the corresponding carboxylic acids (**6a**–**h**, **6j**, **6l**–**o** and **8**) or obtained commercially (**6i** and **6k**), were reacted with the appropriate amines (**1a**–**c**) in the presence of *N*,*N*-diisopropylethylamine at room temperature to afford compounds **7a**–**o**, **9**, and **10** in the yields ranged from 18% to 69%. Deprotection of compounds **7j**, **7m**, and **7o** provided target compounds **11a**–**c**. The final products were evaluated for their inhibitory activity against FGFR1 and the proliferation of FGFR1-amplified H1581 cells.

Table 1. SAR of Core Structure

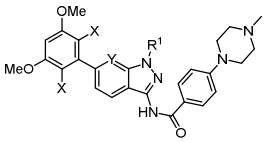

Compd	X	Y	R^1	IC_{50} (nM)[a]		
				FGFR1	VEGF R2	H1581 Cell
9	H	N	H	3709.0 ± 165.3	548.4 ± 94.1	> 1000
4a	Cl	N	H	0.3 ± 0.1	365.9 ± 80.7	1.7 ± 0.2
5	Cl	CH	H	3.3 ± 0.0	ND[b]	324.3 ± 4.6
10	Cl	N	Me	> 5000	ND	ND
AZD4547	-	-	-	1.2 ± 0.1	67.2 ± 3.3	37.9 ± 2.8

[a]Values are the mean ± SD of two independent assays. [b]ND: not determined.

Based on the structure of AZD4547, we utilized the scaffold hopping strategy to design and synthesize compound **9**. Much to our disappointment, **9** showed weak activity against FGFR1 albeit displayed moderate potency against VEGFR2 (IC_{50} = 3709.0 and 548.4 nM, respectively) (Table 1). To enhance its potency and selectivity, we introduced two chlorine atoms to the ortho positions of the dimethoxyphenyl ring (**4a**). To our delight, **4a** exhibited high enzymatic and cellular activities

against FGFR1 (IC_{50} = 0.3 and 1.7 nM, respectively), and had a 1200-fold selectivity for FGFR1 over VEGFR2 (IC_{50} = 365.9 nM) (Table 1). Next, we assessed the importance of the 1*H*-pyrazolo[3,4-*b*]pyridine moiety. Replacement of the 1*H*-pyrazolo[3,4-*b*]pyridine with 1*H*-indazole led to a significant loss in enzymatic potency by 11-fold (Table 1, **5** vs **4a**). In addition, *N*-methylation of 1*H*-pyrazolo[3,4-*b*]pyridine nucleus completely eroded the activity in the enzymatic assay (**10**, IC_{50} > 5 μM), which implied that the N(1)-H of pyrazolopyridine moiety participated in H-bonding interactions within the FGFR1 kinase domain.

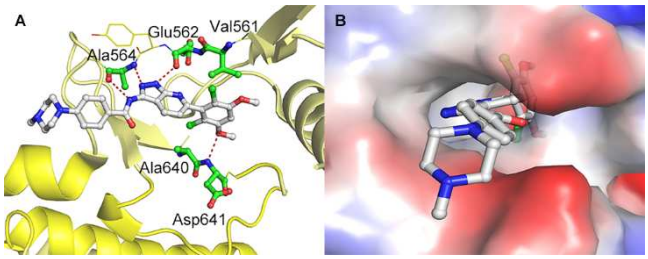

Figure 3. Proposed binding mode of compound **4a** to the FGFR1 kinase domain. The atoms of **4a** are colored as follows: carbon silver, oxygen red, nitrogen blue, and chlorine green. (A) The protein is shown in cartoon and key residues are colored as follows: carbon green, oxygen red, and nitrogen blue. Hydrogen bonds are indicated by red dashes. (B) The protein is shown in surface.

Table 2. SAR of 3-Substituents on 1*H*-Pyrazolo[3,4-*b*]pyridine

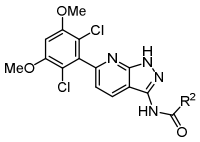

Compd	R^2	IC_{50} (nM)[a]	
		FGFR1	H1581 Cell
4a	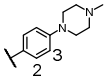	0.3 ± 0.1	1.7 ± 0.2
7a	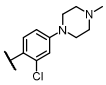	14.0 ± 1.3	27.6 ± 11.0
7b	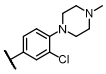	14.5 ± 0.3	191.4 ± 16.7
7c	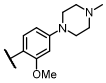	74.4 ± 12.6	525.2 ± 167.0
7d	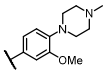	14.2 ± 2.1	15.6 ± 2.6
7e	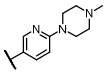	6.2 ± 0.5	1.5 ± 0.4
7f	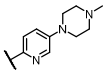	7.8 ± 0.2	4.4 ± 0.2
7g	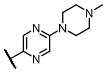	10.5 ± 1.8	60.6 ± 20.7
7h	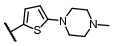	4.1 ± 0.7	3.7 ± 0.3
AZD4547	-	1.2 ± 0.1	37.9 ± 2.8

[a]Values are the mean ± SD of two independent assays.

To elucidate the interaction of 6-(2,6-dichloro-3,5-dimethoxyphenyl)-1*H*-pyrazolo[3,4-*b*]pyridine derivatives with FGFR, we proposed a binding mode of compound **4a** in the ATP site of FGFR1 using a reported crystal structure of the FGFR1 kinase domain (PDB ID: 4WUN). As shown in Figure 3A, **4a** maintained all the H-bonding interactions with FGFR1 observed in AZD4547: the amide NH and the adjacent nitrogen of pyrazolopyridine moiety formed critical H-bonds with the carbonyl and the amino group of Ala564, respectively; the N(1)-H of pyrazolopyridine nucleus was involved in a H-bond with the backbone carbonyl group of Glu562; an additional H-bond occurred between the methoxy oxygen and the amino group of Asp641. Furthermore, the two chlorine atoms, which formed favorable hydrophobic contacts with Val561 and Ala640, respectively, enforced the tetra-substituted phenyl ring to adopt the almost perpendicular orientation with respect to the plane of the pyrazolopyridine rings. Overall, **4a** fitted well into the ATP site of FGFR1, and therefore we chose **4a** as the lead compound for further SAR exploration.

Table 3. SAR of 4-Substituents on Phenyl Ring A

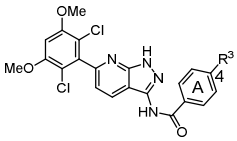

Compd	R^3	IC_{50} (nM)[a]	
		FGFR1	H1581 Cell
4a		0.3 ± 0.1	1.7 ± 0.2
7i	H	42.4 ± 2.9	> 1000
11a	NH_2	8.8 ± 1.2	218.4 ± 1.1
7k	NMe_2	16.5 ± 0.5	294.2 ± 64.7
7l		3.9 ± 0.8	11.0 ± 0.5
11b		11.7 ± 0.8	1.4 ± 0.1
4b		8.8 ± 0.8	558.0 ± 12.8
4c		7.7 ± 0.6	864.8 ± 30.7
4d		6.9 ± 1.1	8.2 ± 1.1
4e		7.2 ± 0.9	1.3 ± 0.2
4f		0.5 ± 0.1	0.7 ± 0.2
4g		1.4 ± 0.1	1.4 ± 0.2
4h		0.2 ± 0.0	2.3 ± 0.2
7n	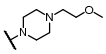	0.3 ± 0.01	0.7 ± 0.1
4i		0.6 ± 0.1	3.3 ± 1.1
11c	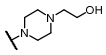	0.3 ± 0.1	< 0.5
4j		0.3 ± 0.1	43.3 ± 1.8
4k		0.2 ± 0.0	244.7 ± 21.6
AZD4547	-	1.2 ± 0.1	37.9 ± 2.8

[a]Values are the mean ± SD of two independent assays.

Table 4. Pharmacokinetic Properties of Compounds 4e, 7n and 11c in ICR Mice[a]

Compd	Dose (mg/kg)	$T_{1/2}$ (h)	C_{max} (ng/mL)	$AUC_{0-\infty}$ (ng·h/mL)	CL (mL/h/kg)	Vd (mL/kg)	F (%)
4e	2 (*iv*)	3.47	869.77	1843.43	1084.93	5427.18	-
	12.5 (*po*)	2.90	499.65	4618.74	-	-	40.21
7n	2 (*iv*)	3.13	825.69	2004.95	997.53	4510.04	-
	12.5 (*po*)	2.76	1648.10	9009.61	-	-	71.95
11c	2 (*iv*)	3.74	796.28	1075.58	1859.47	10025.36	-
	12.5 (*po*)	3.38	801.97	3509.55	-	-	52.30
AZD4547	2 (*iv*)	2.29	1882.86	2076.72	963.06	3175.24	-
	12.5 (*po*)	2.55	1350.03	9127.04	-	-	74.66

[a]n = 3 animals/group. Data are the mean values.

We first examined the impact of various substituents at the C3-position of the pyrazolopyridine scaffold on their biological activity (Table 2). Incorporation of a chlorine atom at the 2- or 3-position of phenyl ring of compound **4a** reduced both enzymatic and cellular potencies (**7a** and **7b**), and the attachment of a methoxy group to the phenyl moiety also resulted in a dramatic drop in potencies (**7c** and **7d**). These results indicated that introduction of either the electron-withdrawing group or the electron-donating group was detrimental to the activity, which could be explained by the fact that the hydrophobic pocket where the phenyl ring was accommodated was too narrow to tolerate any bulky substituent (Figure 3B). In addition, replacement of the phenyl ring with heterocyclic bioisosteres afforded compounds **7e**–**h** with weaker potencies compared to **4a** in both enzymatic and cellular assays. Accordingly, the 2, 3-unsubstituted phenyl ring was optimal for good activity against FGFR1.

Next, we tested the influence of substituents at the 4-position of phenyl ring A on their biological activity (Table 3). Compound **7i** with no substituents on phenyl ring A, showed potent enzymatic potency against FGFR1 with an IC_{50} value of 42.4 nM but poor cellular potency (IC_{50} > 1 μM). Incorporation of an amino group at 4-position of the phenyl ring A improved both enzymatic and cellular potencies (**11a** vs **7i**), and the activity of 4-dimethylamino analogue **7k** was equipotent to that of **11a**. Though 4-(2-(dimethylamino)ethyl)(methyl)amino analogue **7l** displayed a substantial increase in potencies compared to **7k**, it was one order of magnitude less potent than **4a** in both enzymatic and cellular assays. 4-Piperazinyl analogue **11b** was less active in enzymatic assay, but had similar cellular potency compared to **4a**. 4-piperidinyl analogue **4b** and 4-morpholinyl analogue **4c** exhibited comparable enzymatic potency to **11b**, but suffered a large enzyme-to-cell shift. Replacement of the methylpiperazine moiety of **4a** by either methylpiperidine (**4d**) or methylhomopiperazine (**4e**) reduced enzymatic potency, but had little effect on cellular potency. In order to further improve the cellular potency of this series of compounds against FGFR1, various substituents were incorporated at the 4'-position of piperazine moiety of **11b**. Most of the resulting analogues (**4f**–**i**, **7n**, and **11c**) demonstrated excellent inhibitory activity in both enzymatic and cellular assays, except that analogues **4j** and **4k** suffered a sharp enzyme-to-cell shift, perhaps owing to the poor cellular penetration. Thus, a range of substituents were tolerated at the 4'-position of piperazine moiety, presumably because this region extended out of the ATP binding pocket toward solvent (Figure 3).

To assess the pharmacokinetic properties of these 1*H*-pyrazolo[3,4-*b*]pyridine derivatives *in vivo*, we chose compounds **4e**, **7n**, and **11c** for evaluation in male ICR mice through intravenous and oral administration. The key pharmacokinetic parameters are summarized in Table 4. The elimination half-lives ($T_{1/2}$) of compounds **4e**, **7n**, and **11c** were all about three hours after both intravenous and oral administration. The three compounds had similar maximum concentrations (C_{max}) after intravenous administration, while **7n** displayed the highest C_{max} after oral administration. Moreover, AUC values for **7n** were much higher than that for **4e** and **11c** after both intravenous and oral administration, and **7n** had the best oral bioavailability among them. In addition, the *in vitro* plasma protein binding of compounds **4e**, **7n**, **11c** and AZD4547 were determined in mouse plasma, and they all possessed high plasma protein binding rates (99.6%, 99.6%, 99.5%, and 99.3%, respectively). On the basis of its excellent *in vitro* potency and favorable pharmacokinetic properties, **7n** was selected for further evaluation.

Table 5. Kinase Selectivity Profile of Compound 7n

Kinase	IC_{50} (nM)[a]	
	7n	AZD4547
FGFR1	0.3 ± 0.01	1.2 ± 0.1
FGFR2	0.7 ± 0.1	0.4 ± 0.0
FGFR3	2.0 ± 0.3	5.6 ± 1.8
FGFR4	52.7 ± 0.6	45.7 ± 11.2
VEGFR2	422.7 ± 37.6	67.2 ± 3.3

[a]Values are the mean ± SD of two independent assays.

The selectivity of **7n** was evaluated against a panel of 71 protein kinases, including FGFR family (FGFR2–4) and homologous VEGFR2. As depicted in Table 5 and Supporting Information Table S1, **7n** exhibited similar strong potencies against FGFR2 and 3 (IC_{50} = 0.7 and 2.0 nM, respectively) and a moderate potency against FGFR4 (IC_{50} = 52.7 nM). IC_{50} values for all other kinases were more than 1 μM or 400 nM (VEGFR2, IC_{50} = 422.7 nM), indicating **7n** is a selective FGFR1–3 inhibitor.

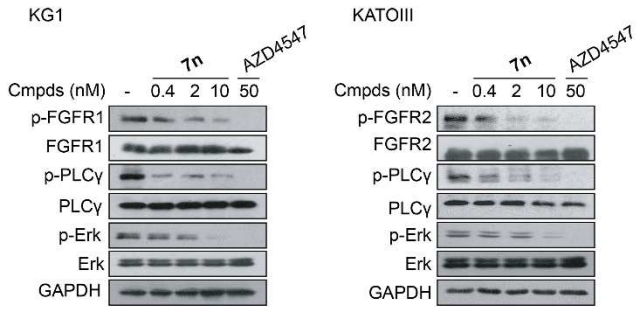

Figure 4. Inhibition of FGFR phosphorylation and downstream signaling by Compound **7n** in KG1 and KATOIII cells.

In Western blot analysis, representative cancer cell lines (KG1, KATOIII) were treated with **7n** and positive drug AZD4547 respectively. As shown in Figure 4, **7n** inhibited the phosphorylation of FGFR1/2 and the phosphorylation of PLCγ and Erk, main downstream effectors of FGFR signaling,[4] in a dose-dependent manner in all the tested cell lines. These results suggested that **7n** exhibited an effective inhibition of FGFR signaling.

Table 6. Effects of Compound 7n on Cell Proliferation

Cell lines	IC_{50} (nM)[a]	
	7n	AZD4547
H1581	0.7 ± 0.1	37.9 ± 2.8
KG1	< 0.2	< 0.2
SNU16	< 0.2	1.2 ± 0.1
KATOIII	< 0.4	20.2 ± 0.5
RT112	< 0.2	0.6 ± 0.3

[a]Values are the mean ± SD of two independent assays.

To elucidate the impact of **7n** on FGFR mediated cancer cell proliferation, five cell lines with known aberrant FGFR activation were chosen, including FGFR1-amplified H1581 cells, FGFR1-translocated KG1 cells, FGFR2-amplified SNU-16 cells and KATOIII cells, and FGFR3-amplified RT112 cells. Compound **7n** showed significantly anti-proliferative effects in all tested cell lines with IC_{50} values less than 1 nM, which was more potent than AZD4547 (Table 6).

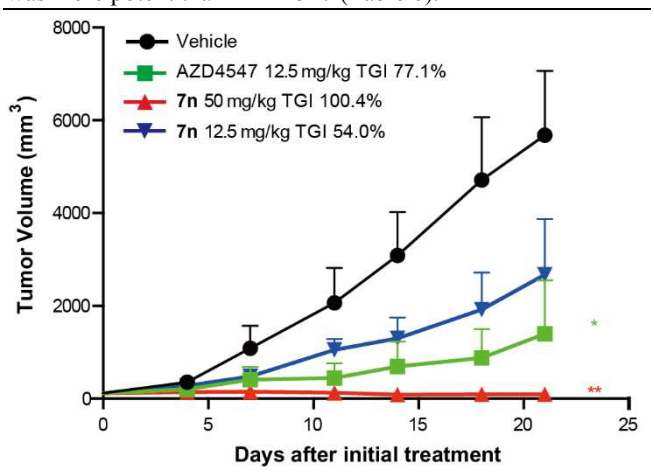

Figure 5. Antitumor efficacy of compound **7n** in H1581 xenograft model. Results are expressed as the mean ± SEM (n = 6 for inhibitor-treated group, n = 12 for vehicle control group).

We finally investigated the *in vivo* antitumor efficacy of **7n** in H1581 xenograft model, which is specifically driven by constitutive activation of FGFR1. Compound **7n** was administered orally at doses of 12.5 mg/kg or 50 mg/kg once daily for 21 consecutive days. The results showed that, compared with the vehicle group, **7n** could suppress tumor growth in a dose-dependent manner, with the tumor growth inhibition rate (TGI) of 54.0% and 100.4% at the doses of 12.5 mg/kg and 50 mg/kg, respectively (Figure 5), without significant body weight loss (see Supporting Information Figure S1).

In summary, we reported the design, synthesis, and biological evaluation of a novel series of 1*H*-pyrazolo[3,4-*b*]pyridine derivatives as potent and selective FGFR kinase inhibitors. Systematic SAR explorations and preliminary assessment of the pharmacokinetic properties resulted in the identification of **7n** as a potential FGFR inhibitor for further evaluation. In addition to excellent potencies against FGFR1–3, **7n** exhibited good selectivity for FGFR over other protein kinases. Besides, the immunoblot analysis revealed that **7n** suppressed FGFR signaling in cancer cells. Moreover, **7n** displayed potent anti-proliferative activities against a number of FGFR-dependent cancer cell lines. Finally, significant antitumor efficacy was observed for **7n** in the FGFR1-driven H1581 xenograft model. All these data indicated that **7n** would be a promising lead compound for further biological evaluation.

ASSOCIATED CONTENT

Supporting Information

The Supporting Information is available free of charge on the ACS Publications website at DOI:
Experimental details for the synthesis of all compounds, biological evaluation, and molecular modeling (Word)

AUTHOR INFORMATION

Corresponding Authors

*(J.A.) E-mail: jai@simm.ac.cn, phone: +86-21-50806600 ext. 2413;
*(M.G.) E-mail: mygeng@simm.ac.cn, phone: +86-21-50806072;
*(W.D.) E-mail: whduan@simm.ac.cn, phone: +86-21-50806032.

Author Contributions

[I]Authors contributed equally to this work.

Funding Sources

We thank the National Natural Science Foundation of China (Nos. 81273365, 81573271, 81473243, and 81321092), National Science & Technology Major Project ''Key New Drug Creation and Manufacturing Program'' (No. 2014ZX09304002-008-001), the Shanghai Science and Technology Commission (No. 1315431901300) for their financial support. SA-SIBS Scholarship Program is also gratefully acknowledged.

Notes

The authors declare no competing financial interest.

ABBREVIATIONS

MAPK, mitogen-activated protein kinase; VEGFR, vascular endothelial growth factor receptor; PDGFR, platelet-derived growth factor receptor; EGFR, epidermal growth factor receptor; DIPEA, *N*,*N*-diisopropylethylamine; THF, tetrahydrofuran; DMF, *N*,*N*-dimethylformamide; TBAF, tetrabutylammonium fluoride; SAR, structure–activity relationship; ATP, adenosine triphosphate; AUC, area under the curve

REFERENCES

(1) Belov, A. A.; Mohammadi, M. Molecular mechanisms of fibroblast growth factor signaling in physiology and pathology. *Cold Spring Harb. Perspect. Biol.* **2013**, *5*, a015958/1–a015958/24.

(2) Laestander, C.; Engström, W. Role of fibroblast growth factors in elicitation of cell responses. *Cell Prolif.* **2014**, *47*, 3–11.

(3) Carter, E. P.; Fearon, A. E.; Grose, R. P. Careless talk costs lives: fibroblast growth factor receptor signalling and the consequences of pathway malfunction. *Trends Cell Biol.* **2015**, *25*, 221–233.

(4) Turner, N.; Grose, R. Fibroblast growth factor signalling: from development to cancer. *Nat. Rev. Cancer* **2010**, *10*, 116–129.

(5) Brooks, A. N.; Kilgour, E.; Smith, P. D. Molecular pathways: fibroblast growth factor signaling: a new therapeutic opportunity in cancer. *Clin. Cancer Res.* **2012**, *18*, 1855–1862.

(6) Knights, V.; Cook, S. J. De-regulated FGF receptors as therapeutic targets in cancer. *Pharmacol. Ther.* **2010**, *125*, 105–117.

(7) Touat, M.; Ileana, E.; Postel-Vinay, S.; André, F.; Soria, J. C. Targeting FGFR signaling in cancer. *Clin. Cancer Res.* **2015**, *21*, 2684–2694.

(8) Greulich, H.; Pollock, P. M. Targeting mutant fibroblast growth factor receptors in cancer. *Trends Mol. Med.* **2011**, *17*, 283–292.

(9) Ho, H. K.; Yeo, A. H.; Kang, T. S.; Chua, B. T. Current strategies for inhibiting FGFR activities in clinical applications: opportunities, challenges and toxicological considerations. *Drug Discov. Today* **2014**, *19*, 51–62.

(10) Ronca, R.; Giacomini, A.; Rusnati, M.; Presta, M. The potential of fibroblast growth factor/fibroblast growth factor receptor signaling as a therapeutic target in tumor angiogenesis. *Expert Opin. Ther. Tar.* **2015**, *19*, 1361–1377.

(11) Lemieux, S.; Hadden, M. K. Targeting the fibroblast growth factor receptors for the treatment of cancer. *Anti-Cancer Agents Med. Chem.* **2013**, *13*, 748–761.

(12) Izzedine, H.; Ederhy, S.; Goldwasser, F.; Soria, J. C.; Milano, G.; Cohen, A.; Khayat, D.; Spano, J. P. Management of hypertension in angiogenesis inhibitor-treated patients. *Ann. Oncol.* **2009**, *20*, 807–815.

(13) Ricciardi, S.; Tomao, S.; de Marinis, F. Toxicity of targeted therapy in non-small-cell lung cancer management. *Clin. Lung Cancer* **2009**, *10*, 28–35.

(14) Guagnano, V.; Furet, P.; Spanka, C.; Bordas, V.; Le Douget, M.; Stamm, C.; Brueggen, J.; Jensen, M. R.; Schnell, C.; Schmid, H.; Wartmann, M.; Berghausen, J.; Drueckes, P.; Zimmerlin, A.; Bussiere, D.; Murray, J.; Graus Porta, D. Discovery of 3-(2,6-dichloro-3,5-dimethoxy-phenyl)-1-{6-[4-(4-ethyl-piperazin-1-yl)-phenylamino]-pyrimidin-4-yl}-1-methyl-urea (NVP-BGJ398), a potent and selective inhibitor of the fibroblast growth factor receptor family of receptor tyrosine kinase. *J. Med. Chem.* **2011**, *54*, 7066–7083.

(15) Gavine, P. R.; Mooney, L.; Kilgour, E.; Thomas, A. P.; Al-Kadhimi, K.; Beck, S.; Rooney, C.; Coleman, T.; Baker, D.; Mellor, M. J.; Brooks, A. N.; Klinowska, T. AZD4547: an orally bioavailable, potent, and selective inhibitor of the fibroblast growth factor receptor tyrosine kinase family. *Cancer Res.* **2012**, *72*, 2045–2056.

(16) Nakanishi, Y.; Akiyama, N.; Tsukaguchi, T.; Fujii, T.; Sakata, K.; Sase, H.; Isobe, T.; Morikami, K.; Shindoh, H.; Mio, T.; Ebiike, H.; Taka, N.; Aoki, Y.; Ishii, N. The fibroblast growth factor receptor genetic status as a potential predictor of the sensitivity to CH5183284/Debio 1347, a novel selective FGFR inhibitor. *Mol. Cancer Ther.* **2014**, *13*, 2547–2558.

(17) Mohammadi, M.; Froum, S.; Hamby, J. M.; Schroeder, M. C.; Panek, R. L.; Lu, G. H.; Eliseenkova, A. V.; Green, D.; Schlessinger, J.; Hubbard, S. R. Crystal structure of an angiogenesis inhibitor bound to the FGF receptor tyrosine kinase domain. *EMBO J.* **1998**, *17*, 5896–5904.

Table of Contents

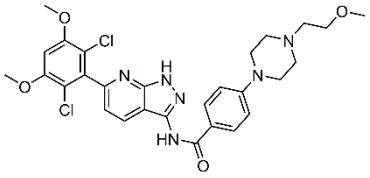

7n

FGFR1-4 IC_{50} = 0.3, 0.7, 2.0, and 52.7 nM
VEGFR2 IC_{50} = 422.7 nM